Mechanical Properties and Morphology of Hot Drawn Polyacrylonitrile Nanofibrous Yarn

S. A. Hosseini Ravandi,[1,2] E. Hassanabadi,[1] H. Tavanai,[1] R. A. Abuzade[1,2]

[1]*Department of Textile Engineering, Isfahan University of Technology, Isfahan 84156-83111, Iran*
[2]*Nanotechnology & Advanced Materials Institute, Isfahan University of Technology, Isfahan 84156 83111, Iran*

Received 7 February 2011; accepted 9 September 2011
DOI 10.1002/app.35602
Published online 11 December 2011 in Wiley Online Library (wileyonlinelibrary.com).

ABSTRACT: In this study PAN nanofibrous yarn was produced by two-nozzle conjugated electrospinning method. The nanofibrous yarns were drawn continuously in boiling water with drawing ratios of 1, 2, 3, and 4. The morphology of drawn yarns was investigated by scanning electron microscopy and tested for tensile properties as well as untreated yarn. The results showed that the nanofiber alignment in the yarn axis direction, the tensile strength, and tensile modulus of yarn increases as a result of drawing while the tensile strain and work of rapture decrease. X-ray diffraction patterns of the produced yarns were analyzed as well. It was found that crystallinity index increases as the draw ratio increases. © 2011 Wiley Periodicals, Inc. J Appl Polym Sci 124: 5002–5009, 2012

Key words: nanofiber; drawing; mechanical properties

INTRODUCTION

Polymeric nanofibers can be produced by a number of techniques such as drawing,[1] template synthesis,[2,3] phase separation,[4] self-assembly,[5,6] and electrospinning.[7,8] Electrospinning is currently the simplest, versatile, applicable, and high potential technique for fabricating continuous nanofibers with diameters down to a few nanometers.[9] In a typical electrospinning setup, a reservoir is used to contain a polymeric solution. The solution is transferred from the reservoir to a spinneret which is generally a blunt tip needle commonly using a syringe pump.[10] A pendant drop of the polymer solution is allowed to form at the needle tip. A high voltage bias is then applied to the solution such that at a critical voltage the electrostatic repulsive forces within the solution will cause a fine jet of solution to erupt from the tip of the pendent drop. The distance between the collector and needle can be adjusted depending on many factors including the ability of the solvent to evaporate although it usually varies between 10 and 20 cm. Although the initial portion of the electrospun jet is stable, this jet soon enters into a bending instability region where further stretching, bending, spiraling, evaporation of the jet, and looping paths with growing amplitude cause the formation of a nonwoven mesh on collector.[11–13]

Correspondence to: S. A. Hosseini Ravandi (hoseinir@cc.iut.ac.ir).

Journal of Applied Polymer Science, Vol. 124, 5002–5009 (2012)

An attractive feature of electrospinning is the simplicity and inexpensive nature of setup.[14] Electrospun nanofiber exhibit a range of unique features and properties that distinguish themselves from nanofiber fabricated using other techniques. Electrospinning has the following advantages: it can produce continuous nanofibers; it can be applied to a wide range of polymers; the dimensions and surface morphologies of the electrospun nanofibers can be varied by altering the solution properties and processing parameters[15]; very large surface area to volume ratio, and superior mechanical performance of the electrospun nanofibers.[16]

The electrospun nanofibers are often collected as randomly oriented structure in the form of nonwoven mats due to the bending instability of the highly charged jet. The electrospun nanofiber is highly charged after they have been ejected from the nozzle, and therefore it is possible to control its trajectory electrostatically by applying an external electric field.[10] The uniaxially aligned arrays of electrospun nanofibers are suitable for applications where isotropic/anisotropic behavior well-aligned and highly ordered architectures for isotropic behaviors are required: these are, for examples, microelectronics, photonics, and blood vessel scaffolds.[17] Even for applications as simple as nanofiber based yarn, it is also critical to control the alignment of nanofibers to improve mechanical performance.[7]

Many trials have been done to advise approaches for collecting electrospun nanofibers as aligned arrays.[18–22] They are a rotating drum collector technique,[23,24] an auxiliary electrode, and electrical field technique,[25,26] a spinning thin wheel with a sharp

edge technique,[27] a frame collector technique,[28–30] and a multiple field technique.[7,30,31]

Many researchers with various disciplinary backgrounds have been worked in this area. Some of them tried to bring the aligned array of nanofiber in a yarn structure. For examples, Fennessey and Farris[32,33] produced discrete lengths of partially aligned and oriented electrospun PAN nanofibers; Wang et al.[34] studied the effects of post-treatment on the mechanical properties of self-bundled electrospun fiber yarns; and Dabirian and Hosseini introduced a new method in which continuous nanofiber yarn can be produced through modified electrospinning.[35,36] Some other researchers tried to enhance mechanical properties of nanofiber. Hosseini et al.[37] studied the structure and mechanical properties of untreated and thermally treated drawn polyacrylonitrile (PAN) nanofiber. Hou et al.[38] investigated the effect of hot-stretching on mechanical properties of as-spun nanofibers. Xu et al.[39] examined the effect of two-stage drawing process on structure and mechanical properties of PAN nanofibers.

In this work, we tried to combine the three main disciplinary explained above to produce aligned nanofiber, incorporate them in a nanofibrous yarn body and enhanced their mechanical properties using hot drawing continuously. To achieve this purpose, PAN nanofibrous yarns were produced by two-nozzle-conjugated electrospinning system. Produced yarns were drawn continuously in boiling water bath. Scanning electron microscopy (SEM) images, mechanical testing, and X-ray diffraction were applied to investigate the structural and mechanical properties of manufactured yarn.

EXPERIMENTAL

Materials

PAN of special grade with weight average molecular weight ($\overline{M_w}$) of 186,000 g/mol was supplied by Poly Acryl, Iran. The solvent used was dimethyl formamide (DMF) from Merck Company, Germany. A polymer solution of 14% (w/w) of PAN/DMF was prepared. The solution was stirred at constant rate at 70°C for 2 h.

Nanofiber yarn formation

Electrospinning setup

Figure 1 schematically illustrates the basic setup for electrospinning and yarn formation. It consists of a high-voltage power supply, two syringe pumps, and a metal cylinder. Two different charged nozzles were placed at 14 cm distance opposite each other and a neutral surface was placed in the middle of them at a distance of 5 cm. The solution was electrospun at applied voltage of 8 kV. The neutral plate induced and the electrospun charged jets moved slightly toward the part of the plate with an opposite charge. At the beginning of the electrospinning process with inserting a piece of yarn in nanofiber path lead to collecting nanofiber on it, then the other end of the nanofiber was pulled toward the plate, making a spinning triangle. It is possible to continuously produce twisted yarn by taking it up during twisting. The take-up unit used can twist and collect yarn simultaneously [Fig. 1(b)].

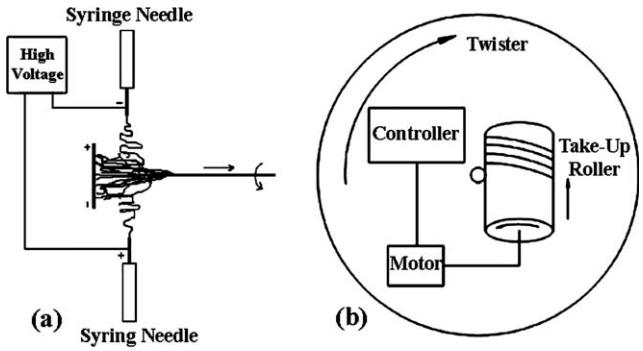

Figure 1 Schematic illustration of (a) yarn formation and (b) take-up unit.[36]

Continuous hot drawing

As an innovative method, manufactured nanofibrous yarn was drawn continuously in boiling water bath equipped with a temperature sensor with accuracy of 0.1°C to prevent the variation of temperature during drawing. Figure 2 schematically illustrate the hot drawing unit. The ratio of drawing was controlled by the speed of a pair of rollers which were placed out of boiling water bath for the draw ratios of 1, 2, 3, and 4. It takes 4 min for yarn to pass through the drawing zone (hot water bath).

Characterization

Mechanical testing

The mechanical properties of manufactured nanofibrous yarn (both as-spun and drawn yarn) were examined using a Zwick 1446-60 in constant rate of elongation mode. To obtain load elongation curves, the sample gauge length of 25 mm and a crosshead speed of 25 mm/min in tension at room temperature were used. The yarns were mounted onto paper tabs similar to that used for single fiber evaluation of conventional sized filaments.

Morphology

The alignment, diameter, and morphology of PAN nanofiber and yarn (as-spun and drawn yarn) were

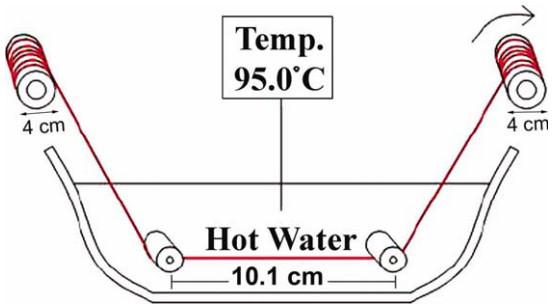

Figure 2 Schematic illustration of continuous hot drawing. [Color figure can be viewed in the online issue, which is available at wileyonlinelibrary.com.]

observed by SEM. Yarns were mounted onto SEM plates; sputter coated with gold, and image registered using a Philips XL30 electron microscope.

X-ray diffraction

X-ray diffraction patterns (intensity vs. diffraction angle plots) were obtained on a Philips (X' Pert MPD, Holland) X-ray diffractometer equipped with a scintillation counter and a chart recorder, with identical setting for all samples. CuK_{α} radiation was used. The nanofiber yarn sample was wrapped closely parallel to each other on the sample holder.

RESULTS AND DISCUSSION

SEM images

To investigate the effect of hot drawing on nanofiber morphology and yarn structure SEM was used. Figure 3 show the scanning electron micrographs of as-spun (not drawn) nanofibrous yarn. The images show poor nanofiber orientation in the yarn axis.

The SEM images of nanofibrous yarn after passing hot water bath (95°C) with no further drawing (draw ratio = 1) are shown in Figure 4. A subjective comparison between SEM images of Figures 3 and 4 represented that wet heating of nanofibrous yarn will lead to some orientation in nanofibers to yarn axis. Moreover, the nanofibrous yarn diameter decreases as a result of wet hot treatment. The shrinkage of nanofibers yarn could be addressed to the decrease of gaps between nanofibers in yarn. In this manner, nanofibers get nearer to each other and lead to decrease in the nanofibrous yarn diameter from 110 down to 80 μm.

Figure 5 show the SEM images of nanofibrous yarn which was drawn in hot water. Hot water treatment and drawing were done simultaneously for various draw ratios. The SEM images show that applying drawing during hot water treatment will cause further nanofiber orientation in the yarn direction. In another word, the angle between nanofibers and the yarn direction decreases. It is shown that higher draw ratio cause higher nanofiber orientation in the yarn axis. For the draw ratio of 4, it can be seen from Figure 5(d) that most of nanofibers came parallel to the yarn axis.

To determine the average diameter of electrospun nanofibers, the annotation and measurement tools on the Motic program were used at 100 different points on the SEM images. Measurements show that increases in draw ratio lead to decrease in nanofiber diameter. For the case with no further draw no significant changes occur in nanofiber diameter. Fiber shrinkage occurs during thermal treatment of PAN fibers due to provided kinetic conditions for molecules to relax strain acquired by stretching during electrospinning. Figure 6 show the manner of nanofiber and nanofibrous yarn diameter variation for various hot draw ratios. The graph shows no significant change in nanofiber diameter for draw ratio of 1, but a drastically decrease from 400 down to 320 nm for draw ratio of two. Higher draw ratios did not lead to further decrease in nanofiber diameter. As explained before, comparing SEM images

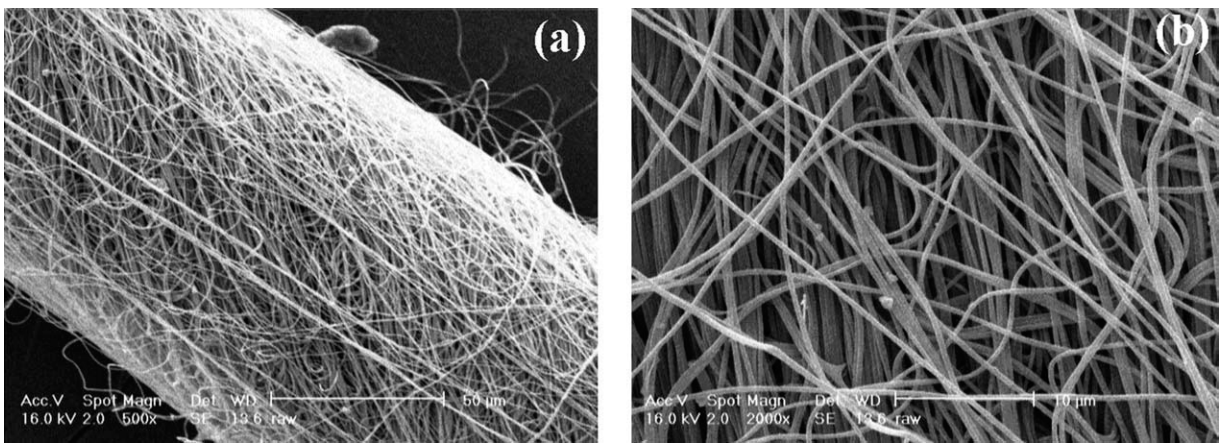

Figure 3 SEM images of as-spun nanofibrous yarn, (a) Magnification ×500, (b) Magnification ×2000.

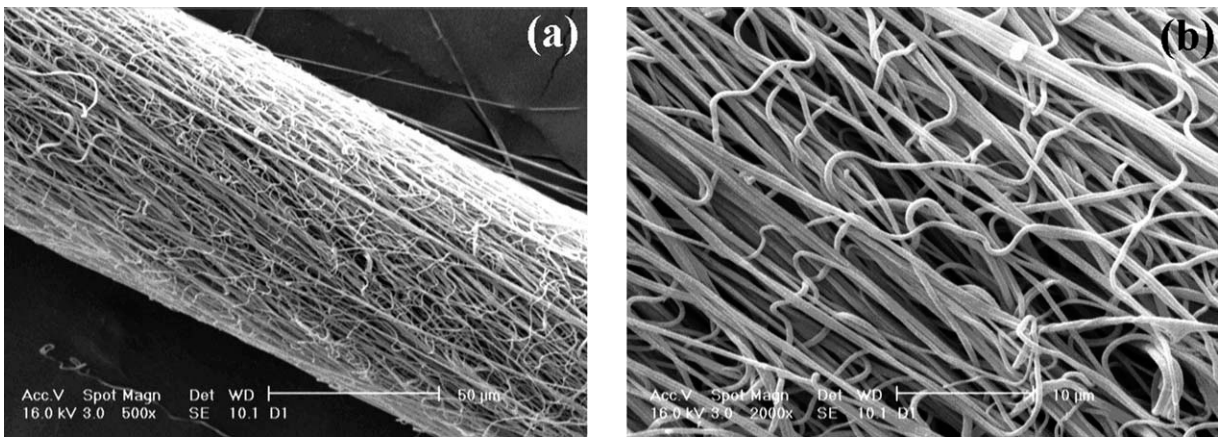

Figure 4 SEM images of nanofibrous yarn after passing hot water bath at 95°C with out any extra drawing, (a) draw ratio = 1, Magnification ×500, and (b) draw ratio = 1, Magnification ×2000.

showed decreases in nanofibrous yarn diameter by increasing draw ratios.

This procedure was examined by measuring nanofibrous yarn diameter. Higher draw ratio values lead to higher nanofiber orientation in the yarn axis; therefore, gaps between nanofibers on the yarn body will decrease. In another word, yarn bulkiness will decrease and dramatic decrease from 110 down to 40 μm will occur in nanofibrous yarn diameter.

Mechanical properties

Linear density of the as-spun and drawn nanofibrous yarns was measured and the results are listed

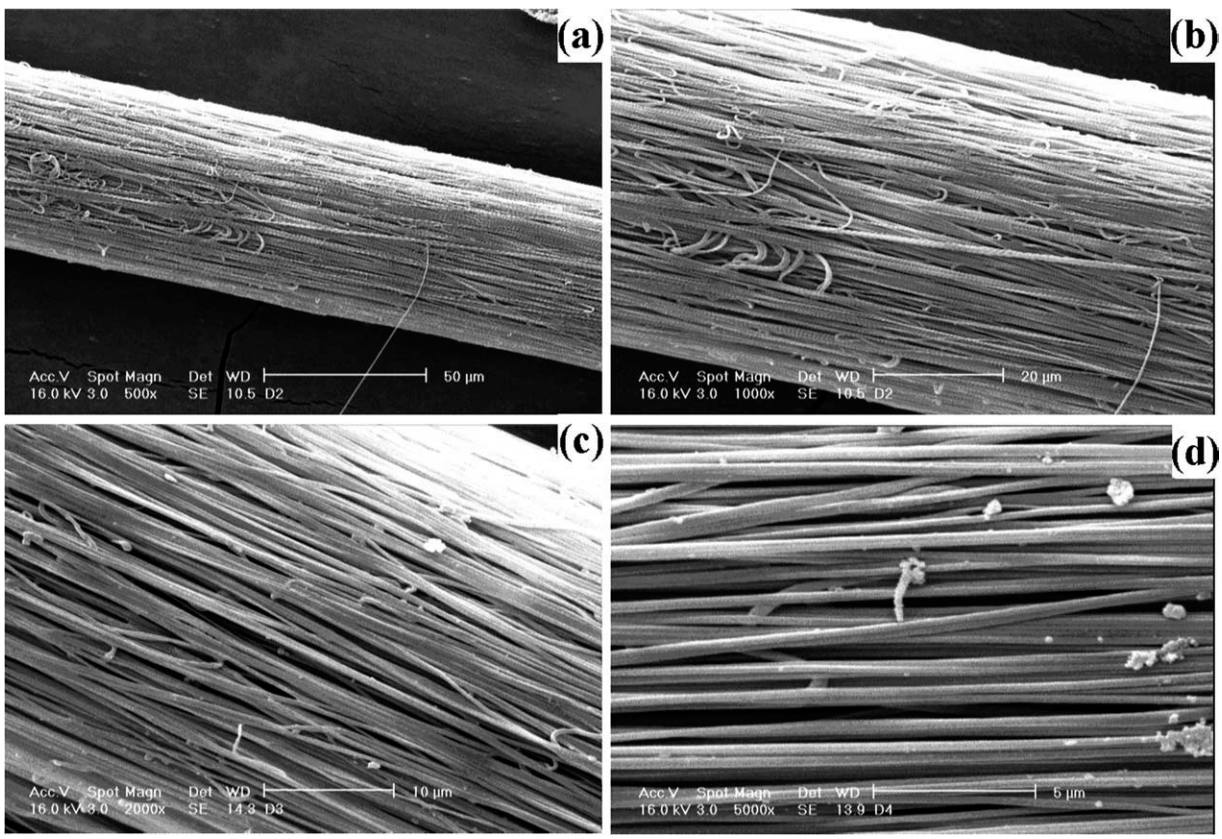

Figure 5 Typical SEM images of nanofibrous yarn after passing hot water bath at 95°C and applying further drawing; (a) draw ratio = 2, magnification = ×500, (b) draw ratio = 2, magnification = ×1000, (c) draw ratio = 3, magnification = ×2000, and (d) draw ratio = 4, magnification = ×5000.

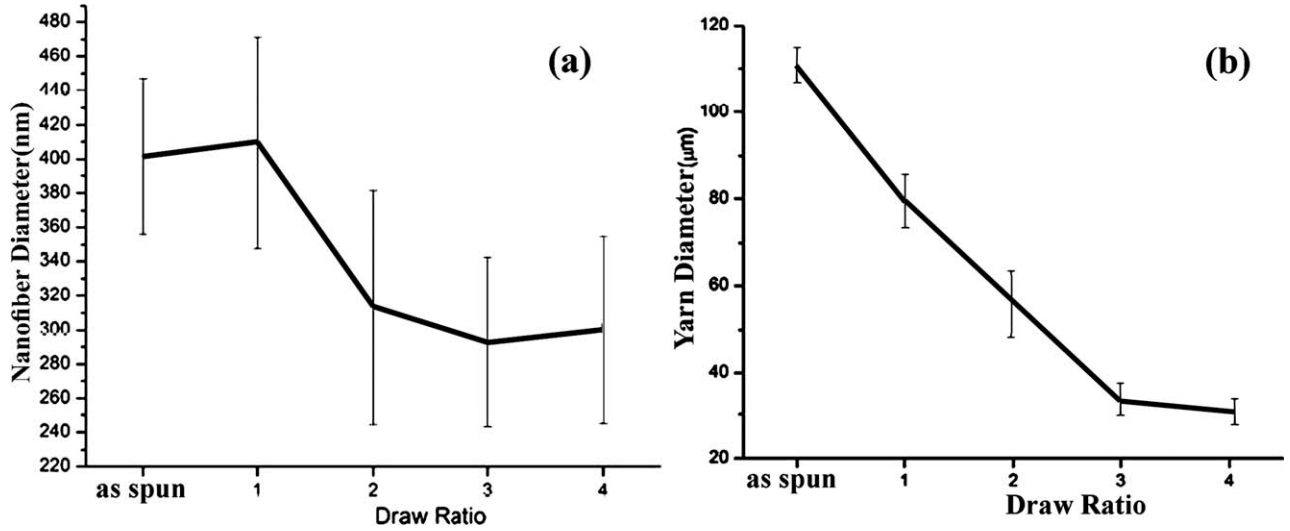

Figure 6 (a) Nanofiber and (b) Nanofibrous yarn diameter for various draw ratios.

in Table I. Comparing the linear densities in various draw ratios showed that there is a considerable difference between mechanical and actual draw ratios. Mechanical draw ratio is set by the ratio of the speed of the delivery roller relative to the feed one, whereas the actual draw ratio is calculated by considering the yarn linear density before and after drawing. A summary of mechanical and actual draw ratios is listed in Table I.

Figure 7(a) shows the tensile strength of as-spun and hot drawn PAN nanofibrous yarns. It is shown that the tensile strength of nanofibrous yarns increases from 80 to 350 MPa with increasing draw ratios. In addition, it is of high interest to note that passing the nanofibrous yarn through the boiling water without any further drawing (draw ratio = 1), increases the tensile strength of the yarn considerably from 50 to 80 MPa. Hot treatment with out further drawing leads to changes in the nanofiber structure as well as a better cohesion of the nanofibers as a result of their shrinkages. It can be said that hot treatment induces a higher degree of structural orientation in the chains of nanofibers. Applying drawing to nanofibrous yarn treated in hot water leads to an increase in the structural orientation of the chains as well as the orientation of nanofibers in the yarn axis direction. The drawing mechanism inherently uncoils the molecular chain to reach higher orientation. The variation of molecular orientation with respect to take-up speed was characterized by polarized Raman spectroscopy in previous study of our research group.[40] As a brief Raman spectra were obtained with a Thermo Nicolt Raman Spectrometer model Almega Dispersive 5555. The spectra were collected in the backscattering mode, using the 532-nm line of a Helium/Neon laser. Raman spectra show a much stronger orientation of the molecular chains in the nanofiber direction for the samples with higher take-up speed and lower orientation for the samples with lower take-up speed. These lead to a more uniform distribution of force on nanofibers in the yarn structure and hence a higher tensile strength of nanofibrous yarn.

Variation of tensile modulus versus draw ratio is shown in Figure 7(b). As can be seen, Young's modulus varied in a manner similar to tensile strength. Statistical analyses such as correlations test confirm the correlation between tensile strength and tensile modulus in all levels.

Yarn strain is the most important property which is generally mentioned after yarn strength. Figure 8(a) shows the variations of strain at break in various draw ratios. It is shown that hot water treatment of nanofibrous yarn with out any further drawing

TABLE I
Characteristics of Drawn Nanofibrous Yarn

Mechanical draw ratio	Linear speed of first roller (cm/min)	Linear speed of second roller (cm/min)	Linear density before drawing (Denier)	Linear density after drawing (Denier)	Actual draw ratio
1	2.53	2.53	39.2	37.9	1.05
2	2.53	5.06	39.2	23.0	1.70
3	2.53	7.59	39.2	10.2	3.80
4	2.53	10.12	39.2	7.7	5.10

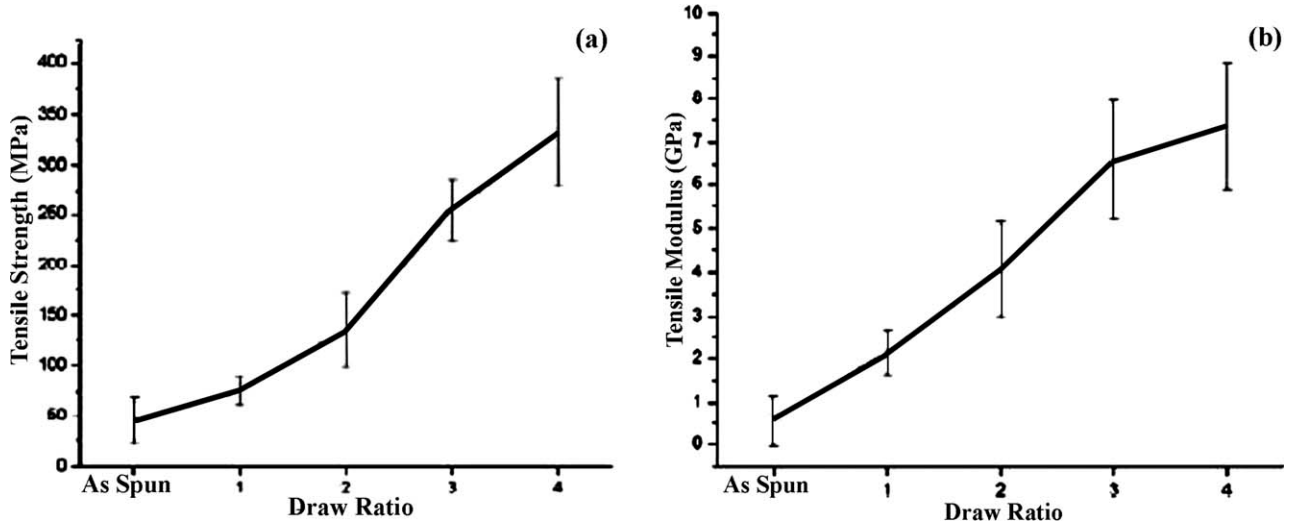

Figure 7 (a) Tensile strength and (b) young's modulus of as-spun and hot drawn nanofibrous yarn.

leads to a considerable decreases from 130 down to 30% in the yarn strain at break. It can be explained by the increasing of the structural orientation of the chains in the nanofiber due to heat treatment. Applying drawing through hot water treatment leads to some decreases from 30 down to 20% in the yarn strain at break. The main decrease in this regime occurs between draw ratios of 1 and 2 and other draw ratios have no dominant role in decreasing the strain at break. It can be explained by the increasing of the nanofiber alignment in the yarn structure due to drawing. Statistical analyses such as analysis of variance (ANOVA) confirm the results at confidence interval of 95%.

It is worthy to evaluate tensile stress and tensile strain simultaneously. Work of rapture will do this evaluation. Figure 8(b) shows the variations of work of rupture in various draw ratios. This manner could be explained by reminding the roles of tensile strength and tensile strain at work of rupture variation. It is obvious that decreasing of strain had more dominant role in comparison with increasing tensile strength and the work of rapture decrease from 5 down to 1 N.mm during the process. ANOVA confirm the results at confidence interval of 95%. The attained mechanical properties can be tied to the higher crystallinity of the nanofibers and better alignment of them in the yarn axis, respectively.

X-ray diffraction

It was shown in our previous research that the crystallinity of as-spun nanofibers is not suitable in electrospinning.[37] This is probably due to rapid evaporation of DMF solvent and low time of nanofiber solidification and as a result, lack of enough

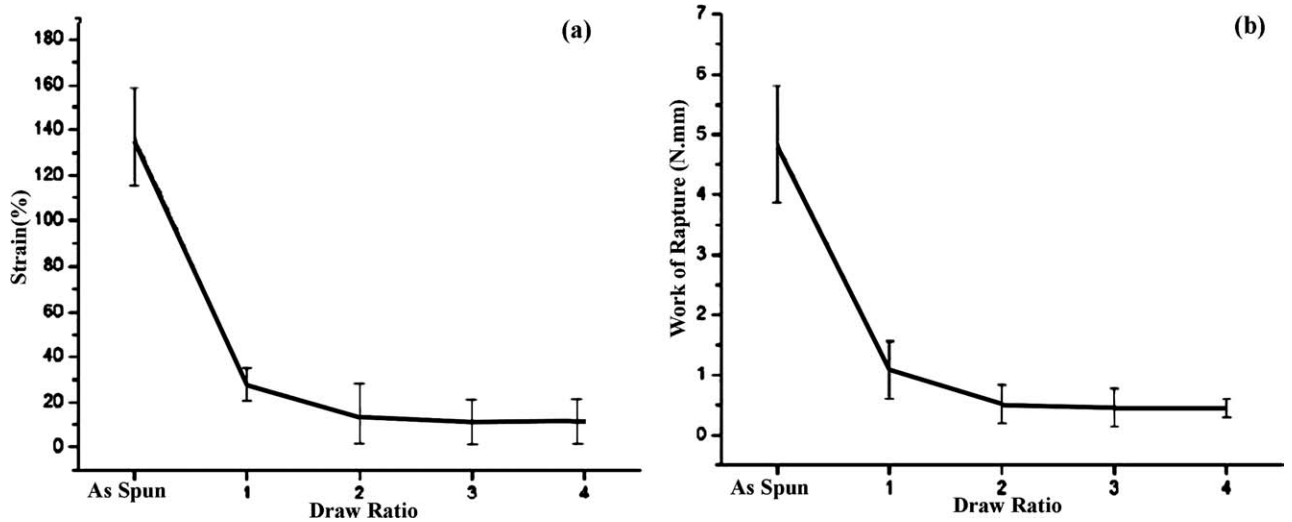

Figure 8 (a) Strain at break and (b) work of rupture of as-spun and hot drawn nanofibrous yarn.

opportunity for organizing molecular chains in ordered crystalline structure.

The wide-angle X-ray diffractograms for the as-spun and hot drawn nanofibrous yarn with draw ratios of 2 and 4 are shown in Figure 9. A strong diffraction peak centered at $2\theta \approx 17$ and a weak diffraction peak centered at $2\theta \approx 29.5$ is a characteristic feature of the X-ray diffraction pattern of PAN reported by various authors. These two peaks represented the X-ray reflection of the (100) and (110) crystallographic planes in PAN.[41,42] The position of the diffraction peaks on the 2θ axis remains unchanged for all the samples in this study and no new reflection seems to occur in drawn samples. This suggests that the crystalline lattice remains unaffected by the hot drawing treatment.

As shown in Figure 9, the as-spun sample exhibited wider pattern, whereas the drawn samples exhibited a sharper pattern. Heating PAN nanofibers at near T_g temperature and drawing of them increases the molecular mobility enough to permit some additional development of the crystalline order. Therefore, the polymeric chains will organize themselves into an arranged crystal structure. It will be expected that by providing sufficient time for polymeric chains, because of the motion of molecular chains in amorphous regains, some smaller crystals might be disturbed while other larger crystals were formed so that the crystallinity of fibers will improved similar to other researches.[43,44] Calculation of crystallinity index (CI) according to the extrapolation of crystal and amorphous parts of the diffraction pattern by the method used by Bell and Dumbleton[45] leads to the value of CI shown in Table II. The CI measured from wide angle X-ray Diffraction (WAXD) patterns of PAN nanofibers has been enhanced with increasing draw ratio.

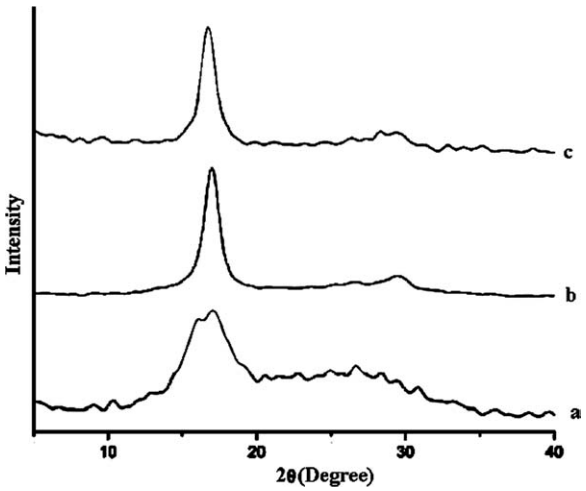

Figure 9 X-ray diffraction plots of PAN nanofibrous yarn (a) as-spun, (b) hot drawn with draw ratio of 2, and (c) hot drawn with draw ratio of 4.

TABLE II
Crystallinity Index (CI) Calculated from X-Ray Diffraction Pattern

Sample	CI %
As spun PAN nanofibrous yarn	27
Hot drawn PAN nanofibrous yarn with draw ratio of 2	44
Hot drawn PAN nanofibrous yarn with draw ratio of 4	64

CONCLUSION

Hot drawing of PAN nanofibrous yarn was done for different draw ratios in 95°C water. Study of SEM images of as-spun and hot drawn PAN nanofibrous yarns result that nanofiber alignment in the yarn axis direction will increase by hot drawing. This causes to better compactness of yarn structure and decrease of yarn diameter. It has been shown that hot drawing increase the tensile strength and tensile modulus; and decrease the tensile strain. It should be noted that there was no significant differences in mechanical properties of hot drawn PAN nanofibrous yarn with draw ratios of 3 and 4. Analyzing the X-ray diffraction plots showed that the intensity of peak at $2\theta = 17$ increased and this peak became sharper. Similarly the CI increased with increasing the draw ratio.

References

1. Ondarcuhu, T.; Joachim, C.; Eur Phys Lett 1998, 42, 215.
2. Martin, C. R. Chem Mater 1996, 8, 1739.
3. Feng, L.; Li, S.; Li, H.; Zhai, J.; Song, Y.; Jiang, L.; Zhu, D. Angew Chem Int Ed 2002, 41, 1221.
4. Ma, P. X.; Zhang, R. J Biomed Mat Res 1999, 46, 60.
5. Liu, G. J.; Ding, J. F.; Qiao, L. J.; Guo, A.; Dymov, B. P.; Gleeson, J. T.; Hashimoto, T.; Saijo, K. Chem A Eur J 1999, 5, 2740.
6. Whitesides, G. M.; Grzybowski, B. Science 2002, 295, 2418.
7. Deitzel, J. M.; Kleinmeyer, J.; Hirvonen, J. K.; Beck, T. N. C.; Polymer 2001, 42, 8163.
8. Smith, L. A. Colloids Surf B Biointerf 2004, 39, 125.
9. Greiner, A.; Wendorff, J. H. Angew Chem Int Ed 2007, 46, 5670.
10. Li, D.; Xia, Y. Adv Mater 2004, 14, 1151.
11. Yarin, A. L.; Koombhongse, S.; Reneker, D. H. J Appl Phys 2001, 89, 3018.
12. Shin, Y. M.; Hohman, M. M.; Brenner, M. P.; Rutledge, G. C. Appl Phys Lett 2001, 78, 1149.
13. Subbiah, T.; Bhat, G. S.; Tock, R. W.; Parameswaran, S.; Ramkumar, S. S. J Appl Polym Sci 2005, 96, 557.
14. Quynh, P. P.; Upma, S. Tissue Eng 2006, 12, 1197.
15. Yang, F.; Kotaki, M. J Biomater Sci Polym Ed 2004, 15, 1483.
16. Huang, Z. M.; Zhang, Y. Z.; Kotaki, M.; Ramakrishna, S. Compos Sci Technol 2003, 63, 2223.
17. Chuangchote, S.; Supaphol, P. J Nanosci Nanotechnol 2006, 6, 125.
18. Bazbouz, M. B.; Stylios, G. K. J Appl Polym Sci 2008, 107, 3023.
19. Moon, S. C.; Choi, J.; Farris, R. J. J Appl Polym Sci 2008, 109, 691.

20. Yang, D.; Zhang, J.; Zhang, J.; Nie, J. J Appl Polym Sci 2008, 110, 3368.
21. Chanunpanich, N.; Byun, H. J Appl Polym Sci 2007, 106, 3648.
22. Pan, H.; Li, L.; Hu, L.; Cui, X. Polymer 2006, 47, 4901.
23. Matthews, J. A.; Wnek, G. E.; Simpson, D. G.; Bowlin, G. L.; Biomacromolecules 2002, 3, 232.
24. Doshi, J.; Reneker, D. H. J Electrost 1995, 35, 151.
25. Bornat, A. US Pat 1987,46,89,186.
26. Berry, J. P. US Pat 1990,49,65,110.
27. Theron, A.; Zussman, E.; Yarin, A. L.; Nanotechnol 2001, 12, 384.
28. Dersch, R.; Liu, T.; Schaper, A. K.; Greiner, A.; Wendorff, J. H. J Polym Sci A 2003, 41, 545.
29. Tan, E. P. S.; Ng, S. Y.; Lim, C. T. Biomaterials 2005, 26, 1453.
30. Li, D.; Wang, Y.; Xia, Y. Nano Lett 2003, 3, 1167.
31. Li, D.; Wang, Y.; Xia, Y. Adv Mater 2004, 16, 361.
32. Fennessey, S. F.; Farris, R. J. Polymer 2004, 45, 4217.
33. Fennessey, S. F.; Pedicini, A.; Farris, R. J. ACS Symp Ser 2006, 918, 300.
34. Wang, X.; Zhang, K.; Zhu, M.; Hsiao, B. S.; Chu, B. Macromol Rapid Commun 2008, 29, 826.
35. Dabirian, F.; Hosseini, Y.; Ravandi, S. A. H. J Text Inst 2007, 98, 237.
36. Dabirian, F.; Hosseini, S. A. Fibres Text East Eur 2009, 74, 45.
37. Jalili, R.; Morshed, M.; Hosseini, S. A. J Appl Polym Sci 2006, 101, 4350.
38. Hou, H. Q.; Ge, J. J.; Zeng, J.; Li, Q.; Reneker, D. H.; Greiner, A.; Cheng, S. Z. D. Chem Mater 2005, 17, 967.
39. Xu, Q.; Xu, L.; Cao, W.; Wu, S. Polym Adv Technol 2005, 16, 642.
40. Sadrjahani, M.; Hosseini, S. A.; Mottaghitalab, V.; Haghi, A. K.; Braz J Chem Eng 2010, 27, 583.
41. Zhou, Z.; Lai, C.; Zhang, L.; Qian, Y.; Hou, H.; Reneker, D. H.; Fong, H. Polymer 2009, 50, 2999.
42. Zussman, E.; Chen, X.; Ding, W.; Calabri, L.; Dikin, D. A.; Quintana, J. P.; Ruoff, R. S. Carbon 2005, 43, 2175.
43. Gupta, V. B.; Kothari, V. K. Manufactured Fiber Technology; Chapman & Hall: London, 1997.
44. Zhang, J.; Huang, L. Q.; Wang, S. Y. J Appl Polym Sci 2006, 101, 787.
45. Gupta, A. K.; Maiti, A. K. J Appl Polym Sci 1982, 27, 2409.